

Published in final edited form as:

J Immunol. 2011 May 15; 186(10): 5543–5547. doi:10.4049/jimmunol.1003865.

Humanized nano pro-resolving medicines mimic inflammation-resolution and enhance wound healing

Lucy V. Norling^{*,†}, Matthew Spite^{*}, Rong Yang^{*}, Roderick J Flower[†], Mauro Perretti[†], and Charles N. Serhan^{*}

^{*} Center for Experimental Therapeutics and Reperfusion Injury, Harvard Institutes of Medicine, Department of Anesthesiology, Perioperative and Pain Medicine, Brigham and Women's Hospital and Harvard Medical School, Boston, MA 02115, USA

[†] William Harvey Research Institute, Barts and the London Medical School, Queen Mary University of London, London EC1M 6BQ, UK.

Abstract

Endogenous microparticles (MPs) were systematically profiled during the time course of self-limited inflammation. Precursors for specialized pro-resolving lipid mediators (LM) were identified in MPs from inflammatory exudates utilizing LC-MS/MS-based metabolomics. Hence, we postulated that formation of anti-inflammatory and pro-resolving LM could underlie beneficial effects attributed to MPs and that this process could serve as a basis for biomimicry. Using human neutrophil-derived MPs, we constructed novel nanoparticles (NPs) containing aspirin-triggered resolvin D1 (AT-RvD1) or a lipoxin A₄ (LXA₄) analog. Enriched NPs dramatically reduced PMN influx in murine peritonitis, shortened resolution intervals and exhibited pro-resolving actions accelerating keratinocyte healing. The enriched NPs protected against inflammation in the temporomandibular joint (TMJ). These findings indicate that humanized NPs, termed nano-pro-resolving medicines (NPRMs) are mimetics of endogenous resolving mechanisms, possess potent beneficial bioactions, can reduce nanotoxicity and offer new therapeutic approaches.

Introduction

Uncontrolled inflammation is a fundamental aetiology of many pathologies, including cardiovascular diseases, arthritis and temporomandibular joint disorders (TMDs) (1, 2). Prevalence of TMDs is high, with at least one symptom afflicting a third of US adults. However, there is an unmet need for effective treatments as options are limited and often involve behavioural or physical therapies or acute administration of nonsteroidal anti-inflammatories (2). Timely resolution of an inflammatory insult is pertinent for restoration of tissue homeostasis and is essential for ongoing health (3). Thus endogenous control mechanisms of inflammation and its resolution are of considerable interest. Recently, potent specialized chemical mediators derived from essential fatty acids were identified that actively promote inflammation resolution via novel pro-resolving and anti-inflammatory cascades (4). Originally, microparticles (MPs) were thought to be inert empty vesicles,

Copyright © [2011] The American Association of Immunologists, Inc.

Address correspondence: Prof. Charles N. Serhan, Director, Center for Experimental Therapeutics and Reperfusion Injury, Department of Anesthesia, Perioperative and Pain Medicine, Brigham and Women's Hospital, Harvard Institutes of Medicine, 77 Avenue Louis Pasteur (HIM 832), Boston, MA 02115, USA **Telephone:** +1-617-525-5001 **Fax:** +1-617-525-5017 cnserhan@zeus.bwh.harvard.edu.

Disclosures C.N.S. is inventor on composition of matter and patents covering lipoxins, resolvins and related compounds owned by BWH-Partners Health Care and licensed for clinical development. C.N.S. retains founder stock in Resolvix Pharmaceuticals.

however, their multiple roles and functional significance during inflammation is now being appreciated. MPs are detected in physiological conditions, with increased numbers disseminated in multiple diseases including rheumatoid arthritis (5). Along these lines, anti-inflammatory properties of MPs shed from polymorphonuclear cells (PMNs) were uncovered (6, 7).

Herein, we investigated the temporal generation and properties of endogenous MPs produced in evolving self-limited inflammatory exudates *in vivo* and constructed a novel biomimetic system utilizing human PMN-derived MPs to stimulate resolution of inflammation as demonstrated in temporomandibular joint disease (TMJ). This biomimetic construction is highly advantageous as compared with other synthetic nanoparticle drug delivery systems that have adverse immunotoxic effects (8).

Materials and Methods

Endogenous microparticles

Peritonitis was initiated in male FVB mice (6-8wk, Charles River) with zymosan A (1mg i.p.) and peritoneal lavages were collected at indicated times. Exudate MPs were isolated by removal of leukocytes (4000g, 15min) followed by ultracentrifugation (100,000g, 1h) and quantified by flow cytometry. MPs were characterized with anti-CD11b (M1/70), CD54 (YN1), isotype control Abs (eBioscience) or CD45 (30-F11) (BD Biosciences) and annexinA5 (BD Biosciences) for external phosphatidylserine. For solid-phase extraction and LC-MS/MS based analyses cold methanol was added to MPs (9).

Preparation of Humanized Nano-Pro-Resolving Medicines (NPRMs)

Human MPs were prepared (6), and added to thin lipid films in glass flasks (after organic solvent removal by rotary evaporation; 10min, 25°C) containing fluorescent 1,2-dioleoyl-sn-glycero-3-phospho-L-serine-N-7-nitro-2-1,3-benzoxadiazol-4-yl (100µg, Avanti Polar Lipids) and 7*S*, 8*R*, 17*R*-trihydroxy-docosa-4*Z*,9*E*,11*E*,13*Z*,15*E*,19*Z*-hexaenoic acid (AT-RvD1; 1µg, Cayman Chemical) or *o*-[9,12]-benzo- ω 6-epi-LXA₄ (1µg) (10) prepared for these studies by contract custom synthesis. Intercalation of AT-RvD1 or LXA₄ analog and fluorescent phospholipid was performed by aqueous energy dissemination using a sonic dismembrator (output power 15W, 15min, 25°C, Fisher Scientific). Humanized nanoparticles (NPs) were layered on Sephadex G50 columns (Sigma) and fractions collected in 0.2µm-filtered PBS. Incorporation of AT-RvD1 and LXA₄ analog were determined using LC-MS/MS, and fluorescent phospholipid content confirmed by flow cytometry (BD FACSCanto II). NPs and MPs were sized using calibration beads (Corpuscular) by flow cytometry and conventional electron microscopy following negative staining (Tecnai™ G² Spirit BioTWIN; HMS core facility).

Mediator Lipidomics

LC/UV/MS/MS-based mediator lipidomics analysis was performed with an HPLC (Shimadzu LC20AD) -UV (Agilent 1100) coupled to a quadrupole ion-trap mass spectrometer (QTrap3200; Applied Biosystems) equipped with a C18 column (Agilent Eclipse Plus, 4.6mm × 50mm × 1.8µm). Acquisition was conducted in negative ionization mode and LM were profiled using scheduled multiple reaction monitoring with identified using retention time, >5-6 diagnostic ions and matching criteria (9). Esterified monohydroxy-products were assessed in endogenous MPs following methanol/chloroform extraction of phospholipids and overnight saponification with 1N potassium hydroxide in 90% ethanol. Samples were acidified and extracted with added internal standard d₅-17-HDHA (1ng) for LC-MS/MS based lipidomics as above.

For MP phosphatidylcholine analyses, LC-UV/MS/MS-based mediator lipidomic analysis was performed with an HPLC (Shimadzu LC20AD) connected inline with a UV diode array detector (Agilent G1315B), coupled to a hybrid quadrupole time-of-flight mass spectrometer (QStar XL; Applied Biosystems) equipped with a Phenomenex Luna C18(2) column (2mm × 150mm × 3μm). Mobile phase consisted of 0.5% ammonium hydroxide in methanol/ acetonitrile/ and 0.1M ammonium acetate (97:2:1;v/v/v) at 200μl/min. Operating parameters and collision energies were optimized individually.

Peritonitis and wound healing

Human MPs or NPRMs (1×10^4 - 3×10^5) were given i.v. (or i.p. as indicated) prior to zymosan A (0.1mg i.p) and peritoneal leukocytes were assessed at 2, 4 or 12h. In some experiments mice were given d₅-DHA (1μg i.v.) prior to zymosan A (1mg), and peritoneal MPs were collected at 4h. Wound healing was assessed using an Electric Cell-substrate Impedance Sensing (ECIS) 1600R system (Applied Biophysics) (11). Human epidermal keratinocytes (Lonza) were cultured on 8W1E electrode arrays, and once confluent (~8,000 Ω; using 16kHz) were wounded (64kHz, 30s). Cells were treated with buffer alone, AT-RvD1 NPRMs (10nM), AT-RvD1 (10nM) or equivalent nanoparticle number.

Temporomandibular joint (TMJ) inflammation

Mice were anesthetized (O₂:1L/min, isoflurane 2.5%), and Complete Freund's adjuvant (CFA) was administered (10μg; 20μl) into the periarticular space of the left TMJ and 0.9% sterile saline (20μl) into the right TMJ space as in (12). Treatments were then delivered i.v. with buffer (100μl PBS), AT-RvD1 (10ng) NPRMs or α -[9,12]-benzo- ω 6-epi-LXA₄ (10ng) NPRMs. After 12h PMN infiltration was assessed in the TMJ by myeloperoxidase (MPO) activity by ELISA (Hycult Biotechnology).

Statistics

Data are mean ± S.E.M. Multiple group comparisons were made using oneway ANOVA followed by Dunnett's or Bonferroni post hoc analysis. $p < 0.05$ was considered significant.

Results and Discussion

First, we profiled the time-course of MP generation in self-limited acute inflammation, i.e. zymosan-induced peritonitis. The endogenous leukocyte-derived MPs were temporally generated *in vivo* in inflammatory exudates, with maximum MPs identified within the initiation phase, which gradually declined during the resolution phase corresponding with neutrophilic loss (Fig 1A). Further characterization of these annexin A5⁺ MPs by surface molecule expression demonstrated these were CD11b⁺, CD45⁺ and CD54⁺ (Fig 1B). To systematically address the lipid mediator (LM) profiles carried by endogenous MPs, liquid chromatography tandem mass spectrometry (LC-MS/MS)-based metabolomics was performed. We discovered that endogenous MPs formed in inflammatory exudates contain esterified biosynthetic precursors of novel specialized pro-resolving mediators (Fig 2A). For example, the levels of MP-associated hydroxydocosahexaenoic acids; namely 14-HDHA and 17-HDHA were high during the initiation phase of acute inflammatory response, decreased during the peak of inflammation and accumulated in resolution, the phase in which potent anti-inflammatory and pro-resolving LM are biosynthesized (13). Fig 2B shows a representative mass spectrum of 17-HDHA, with the diagnostic ions used for identification criteria denoted, including mass-to-charge ratio (m/z) 245 and 273. Notably, endogenous MPs were devoid of unesterified monohydroxy fatty acids, suggesting that once liberated from MP membranes, they are made available to leukocytes within the exudate.

Following *i.v.* administration of deuterium-labelled d_5 -DHA for tracking, circulating d_5 -DHA is made rapidly available to exudates (14) and was incorporated into endogenous MPs generated during the onset of acute inflammation. Additionally, these MPs also contained enzymatic metabolites of d_5 -DHA, namely d_5 -17-HDHA and d_5 -14-HDHA, deuterated biosynthetic pathway biomarkers for D-series resolvins and maresin biosynthesis respectively, which reflects activation of these new pathways and their H(p)DHA intermediates (Fig 2C). These results implicate endogenous MPs as intercellular communicators that can deliver pro-resolving LM precursors to inflammatory loci. Further experiments were performed to assess whether exogenous DHA was stored within MP phospholipids. When human PMN were incubated with d_5 -DHA, MPs were generated containing both d_5 -DHA and d_5 -HDHA esterified into phosphatidylcholine (Supplemental Fig S1A, B). Noteworthy, both cytosolic and secretory PLA₂ are induced during the resolution phase of inflammation (15). sPLA₂ added to resolving MP liberated esterified precursors from MPs (Supplemental Table I).

Human PMN-derived MPs display anti-inflammatory properties via ALX/FPR2, the receptor for LXA₄, annexin-A1 as well as Resolvin D1 (RvD1) (6, 16). Additionally, we demonstrated herein that MPs enhanced efferocytosis (Supplemental Fig 2) and contain precursors for pro-resolving LM, thus likely contributing to the beneficial properties attributed to these MPs. Since many biomaterials used for nanoparticle drug delivery can activate the circulatory system and cause nanotoxicity, for example by uptake and activation of dendritic cells (8), we sought new means to locally administer and activate pro-resolving cascades *in vivo* based on the endogenous MP system. Thus, newly constructed nanomedicines should possess multi-pronged agonist actions in resolution, activating endogenous ALX, releasing precursors for local pro-resolving mediators as well as delivering their cargo of uploaded LM.

Harnessing human neutrophil-derived MPs as scaffolds, we constructed NPs containing either aspirin-triggered resolvin D1 (AT-RvD1) (4) or a stable analog of LXA₄ (10). Following enrichment procedures and energy induced conversion of MP to NPs, preparations were layered onto size-exclusion chromatography columns to separate free unincorporated lipids from MP-associated lipids, and eluate fractions were collected and taken for analyses including flow cytometry. Characteristically, enriched NPs (Fig 3A, blue dot plot) were smaller than their MP counterparts (Fig 3A, red dot plot) and also contained fluorescent phospholipid (Fig 3B, blue histogram). Nanoparticle sizing was accomplished by flow cytometry using nanosphere calibration beads (Fig 3C & D). Sizing was further validated using negative stain electron microscopy of MPs (Fig 3E) and NPRMs (Fig 3F). Both methods showed smaller, more uniform sizing of NPs following enrichment procedures. Prior to each experiment, incorporation of AT-RvD1 or the LXA₄ analog was determined using LC-MS/MS. Representative tandem mass spectrum of nanoparticle associated AT-RvD1 (m/z 375.2) is shown from scheduled multiple reaction monitoring (MRM) of the m/z 375.2/215 transition pair at 7.4min (Fig 3G).

These humanized NPs were inherently anti-inflammatory, even without enriching with LM, counter-regulating PMN infiltration in acute zymosan (0.1mg) peritonitis by ~25% following *i.v.* administration of 1×10^5 NPs (Fig 4A). A similar reduction in PMN influx was observed with 300ng of a stable LXA₄ analog consistent with earlier findings (17). Remarkably, when the LXA₄ analog was incorporated into human NPs, they drastically limited PMN numbers by ~60% showing they possess additional anti-inflammatory properties. Importantly, 1×10^5 NPs equated to an incorporation of 5.0-8.8ng of LX analog, effectively demonstrating that much lower amounts were needed locally to reduce PMN infiltration than analog alone. This proved dose dependent, with maximal NPRMs greatly limiting PMN recruitment (Supplemental Fig 3A). Noteworthy, we found an inhibitory

action on PMN recruitment when NPRMs were administered directly into the peritoneum, suggesting a direct action on resident macrophages, dampening their inflammatory response to zymosan (Supplemental Fig 3B). We also assessed bioactivity of AT-RvD1 enriched NPs in murine peritonitis. Leukocyte recruitment and differential analyses were assessed at 3 separate intervals in order to quantify acute inflammatory response using self-limited inflammation (Fig 4B). Local microbial administration resulted in a rapid increase in PMN infiltration, which peaked at 4h post-challenge corresponding to the onset of inflammation. By 12h PMNs had declined, and the resolution interval (R_i) was calculated (i.e. time taken for maximal PMN to decrease 50%). NPs carrying AT-RvD1 drastically reduced PMN recruitment in microbial peritonitis, reducing maximal PMN infiltration from $9.4 \pm 0.7 \times 10^6$ to $4.0 \pm 0.8 \times 10^6$ and also shortened R_i from 7h to ~4.5h (Fig 4B).

Pro-resolving bioactions of these humanized nanomedicines were next evaluated in a keratinocyte wound-healing assay using *in vitro* epidermal abrasion (11). Following focal clearance of keratinocytes with an elevated electrical field pulse, keratinocyte healing from the perimeter into the clearance zone was assessed in real-time by impedance sensing. This highly sensitive method indicated that AT-RvD1 containing nanomedicines enhanced wound closure rates as compared with either non-enriched NPs or with equimolar amounts of AT-RvD1 (10nM), demonstrating their pro-resolving properties (Fig 4C).

Temporomandibular joint disorders are a significant clinical problem, causing craniofacial pain (2). Effective treatment of pain arising from inflammation of joints and muscles remains an unmet medical need, and is implicated not only in TMDs but also in many other human diseases. To this end, we evaluated whether these nanomedicines would confer protection against CFA-induced inflammation of the TMJ. Indeed, 10ng of either AT-RvD1 NPRMs or α -[9,12]-benzo- ω 6-epi-LXA₄ NPRMs drastically reduced the number of infiltrating PMN into the inflamed TMJ 12h after CFA-induced inflammation (Fig 4D). Importantly, MPO levels in the contralateral TMJ were not elevated, and no significant differences were noted between buffer control and NPRM treatment groups (not shown). Of relevance, both RvD1 and RvE1 also attenuate inflammatory pain (18). Together these results establish that biomimicking endogenous resolution mechanisms centred on anti-inflammatory and pro-resolving MPs, enhances the bioactions of potent LM. Nanoparticle delivery of AT-RvD1 or a stable analog of LXA₄ prevented excessive neutrophilic infiltration to inflamed TMJs thus circumventing ensuing granuloma formation and further joint destruction associated with overzealous leukocyte recruitment in this complex joint disease.

Supplementary Material

Refer to Web version on PubMed Central for supplementary material.

Acknowledgments

We thank Maria Ericsson for expert electron microscopy analysis (HMS core facility), and Khalil Nasser for technical assistance.

This work was supported by National Institutes of Health grants DE 019938 (L.V.N. and C.N.S.) and GM38765 (C.N.S.), Arthritis Research UK fellowship 18445 (L.V.N) and Wellcome Trust Programme grant 086867/Z/08/Z (M.P. and R.J.F.).

References

1. Nathan C, Ding A. Nonresolving inflammation. *Cell*. 2010; 140:871–882. [PubMed: 20303877]

2. Scrivani SJ, Keith DA, Kaban LB. Temporomandibular disorders. *N Engl J Med*. 2008; 359:2693–2705. [PubMed: 19092154]
3. Gilroy DW, Lawrence T, Perretti M, Rossi AG. Inflammatory resolution: new opportunities for drug discovery. *Nat Rev Drug Discov*. 2004; 3:401–416. [PubMed: 15136788]
4. Serhan CN. Resolution phase of inflammation: novel endogenous anti-inflammatory and proresolving lipid mediators and pathways. *Annu Rev Immunol*. 2007; 25:101–137. [PubMed: 17090225]
5. Boilard E, Nigrovic PA, Larabee K, Watts GF, Coblyn JS, Weinblatt ME, Massarotti EM, Remold-O'Donnell E, Farndale RW, Ware J, Lee DM. Platelets amplify inflammation in arthritis via collagen-dependent microparticle production. *Science*. 2010; 327:580–583. [PubMed: 20110505]
6. Dalli J, Norling LV, Renshaw D, Cooper D, Leung KY, Perretti M. Annexin 1 mediates the rapid anti-inflammatory effects of neutrophil-derived microparticles. *Blood*. 2008; 112:2512–2519. [PubMed: 18594025]
7. Gasser O, Schifferli JA. Activated polymorphonuclear neutrophils disseminate anti-inflammatory microparticles by ectocytosis. *Blood*. 2004; 104:2543–2548. [PubMed: 15213101]
8. Hess H, Tseng Y. Active intracellular transport of nanoparticles: opportunity or threat? *ACS Nano*. 2007; 1:390–392. [PubMed: 19206658]
9. Serhan CN, Lu Y, Hong S, Yang R. Mediator lipidomics: search algorithms for eicosanoids, resolvins, and protectins. *Methods Enzymol*. 2007; 432:275–317. [PubMed: 17954222]
10. Petasis NA, Keledjian R, Sun YP, Nagulapalli KC, Tjonahen E, Yang R, Serhan CN. Design and synthesis of benzo-lipoxin A4 analogs with enhanced stability and potent anti-inflammatory properties. *Bioorg Med Chem Lett*. 2008; 18:1382–1387. [PubMed: 18249111]
11. Keese CR, Wegener J, Walker SR, Giaever I. Electrical wound-healing assay for cells in vitro. *Proc Natl Acad Sci U S A*. 2004; 101:1554–1559. [PubMed: 14747654]
12. Kramer PR, Kerins CA, Schneiderman E, Bellingher LL. Measuring persistent temporomandibular joint nociception in rats and two mice strains. *Physiol Behav*. 2010; 99:669–678. [PubMed: 20152846]
13. Serhan CN, Yang R, Martinod K, Kasuga K, Pillai PS, Porter TF, Oh SF, Spite M. Maresins: novel macrophage mediators with potent antiinflammatory and proresolving actions. *J Exp Med*. 2009; 206:15–23. [PubMed: 19103881]
14. Kasuga K, Yang R, Porter TF, Agrawal N, Petasis NA, Irimia D, Toner M, Serhan CN. Rapid appearance of resolvin precursors in inflammatory exudates: novel mechanisms in resolution. *J Immunol*. 2008; 181:8677–8687. [PubMed: 19050288]
15. Gilroy DW, Newson J, Sawmynaden P, Willoughby DA, Croxtall JD. A novel role for phospholipase A2 isoforms in the checkpoint control of acute inflammation. *FASEB J*. 2004; 18:489–498. [PubMed: 15003994]
16. Krishnamoorthy S, Recchiuti A, Chiang N, Yacoubian S, Lee CH, Yang R, Petasis NA, Serhan CN. Resolvin D1 binds human phagocytes with evidence for proresolving receptors. *Proc Natl Acad Sci U S A*. 2010; 107:1660–1665. [PubMed: 20080636]
17. Sun YP, Tjonahen E, Keledjian R, Zhu M, Yang R, Recchiuti A, Pillai PS, Petasis NA, Serhan CN. Anti-inflammatory and pro-resolving properties of benzo-lipoxin A(4) analogs. *Prostaglandins Leukot Essent Fatty Acids*. 2009; 81:357–366. [PubMed: 19853429]
18. Xu ZZ, Zhang L, Liu T, Park JY, Berta T, Yang R, Serhan CN, Ji RR. Resolvins RvE1 and RvD1 attenuate inflammatory pain via central and peripheral actions. *Nat Med*. 2010; 16:592–597. 591p following 597. [PubMed: 20383154]

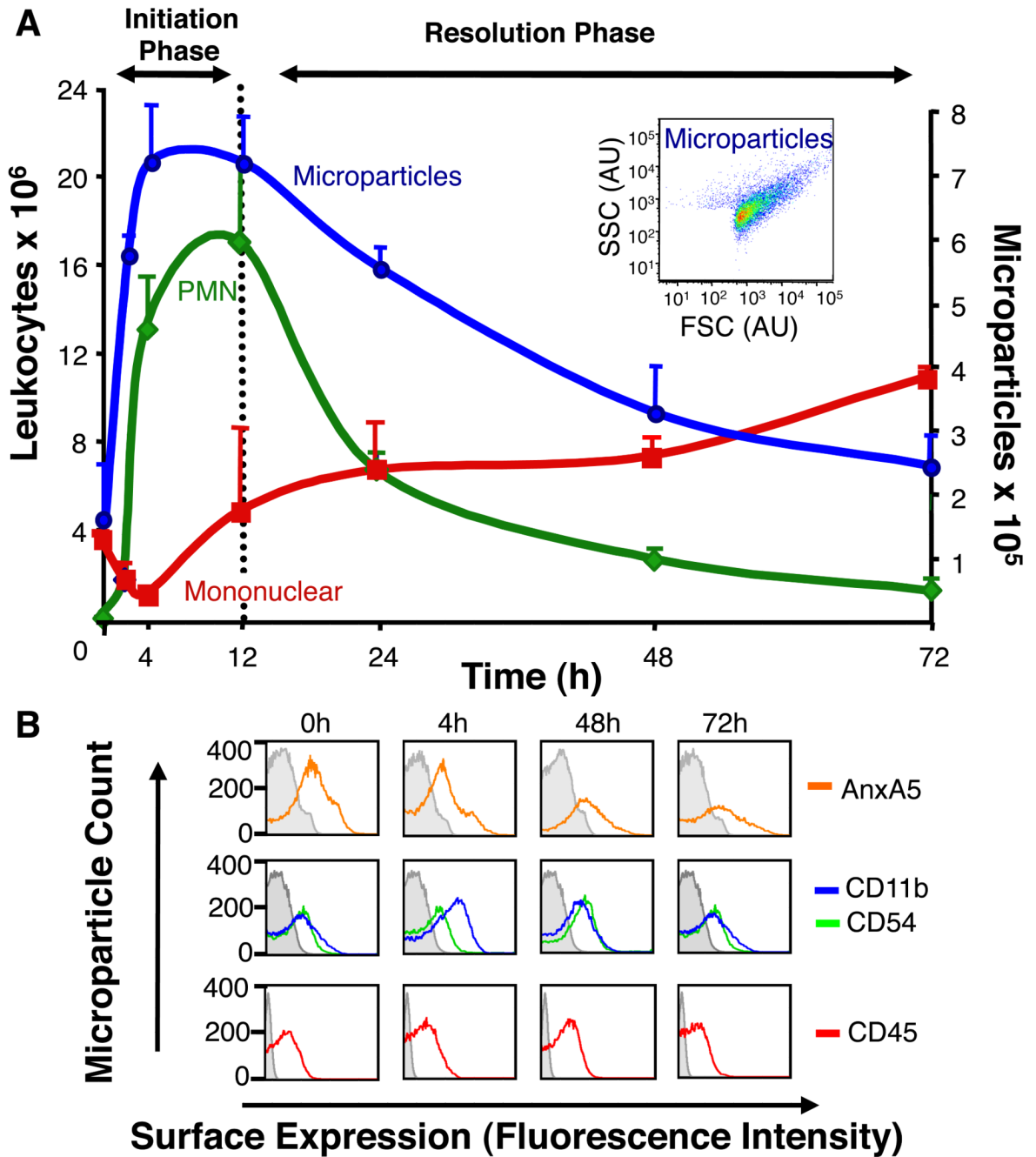


Figure 1. Temporal Production of Endogenous leukocyte-derived microparticles during peritonitis
 (A) Time course of PMN and mononuclear cell accumulation, and MP generation following zymosan-induced murine peritonitis (1mg i.p). *Inset:* Representative 4h MP flow cytometry plot. (B) Characterisation of endogenous MPs from exudates at indicated time points. Results are mean ± SEM (*n*=3-7 per time point).

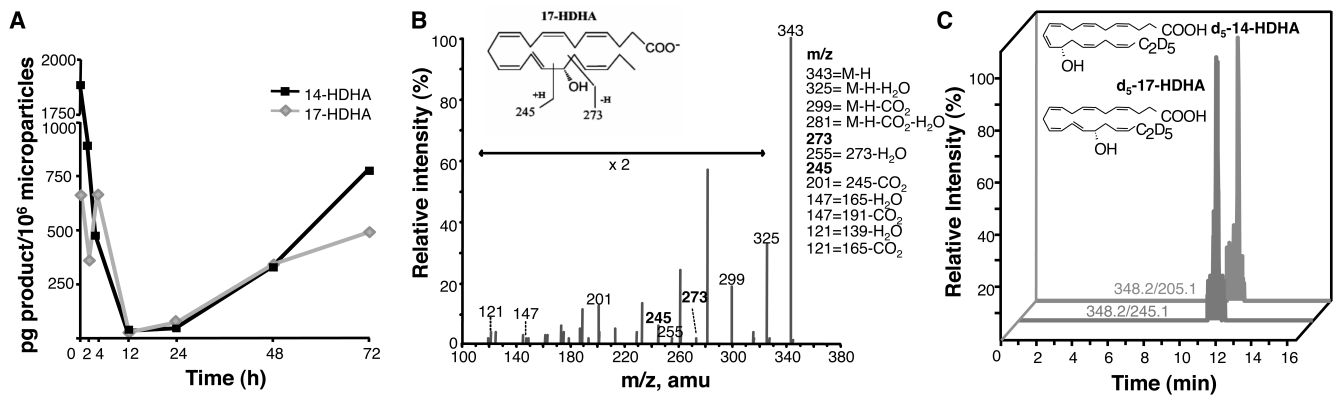


Figure 2. Endogenous leukocyte-derived microparticles contain resolvins precursors and LM pathway markers

(A) MPs collected from zymosan (1mg i.p.) exudates and extracted for targeted lipidomics. LM biosynthetic pathway markers 17-HDHA (grey) and 14-HDHA (black) identified using scheduled MRM. (B) Representative mass spectrum of 17-HDHA within endogenous MPs. (C) Mice were administered d₅-DHA (1μg i.v.) followed by zymosan (1mg i.p.) and MPs collected from 4h lavages. Both d₅-17-HDHA and d₅-14-HDHA were identified (transition pairs 348.2/245.1 and 348.2/205.1). Representative of *n*=3 per time point.

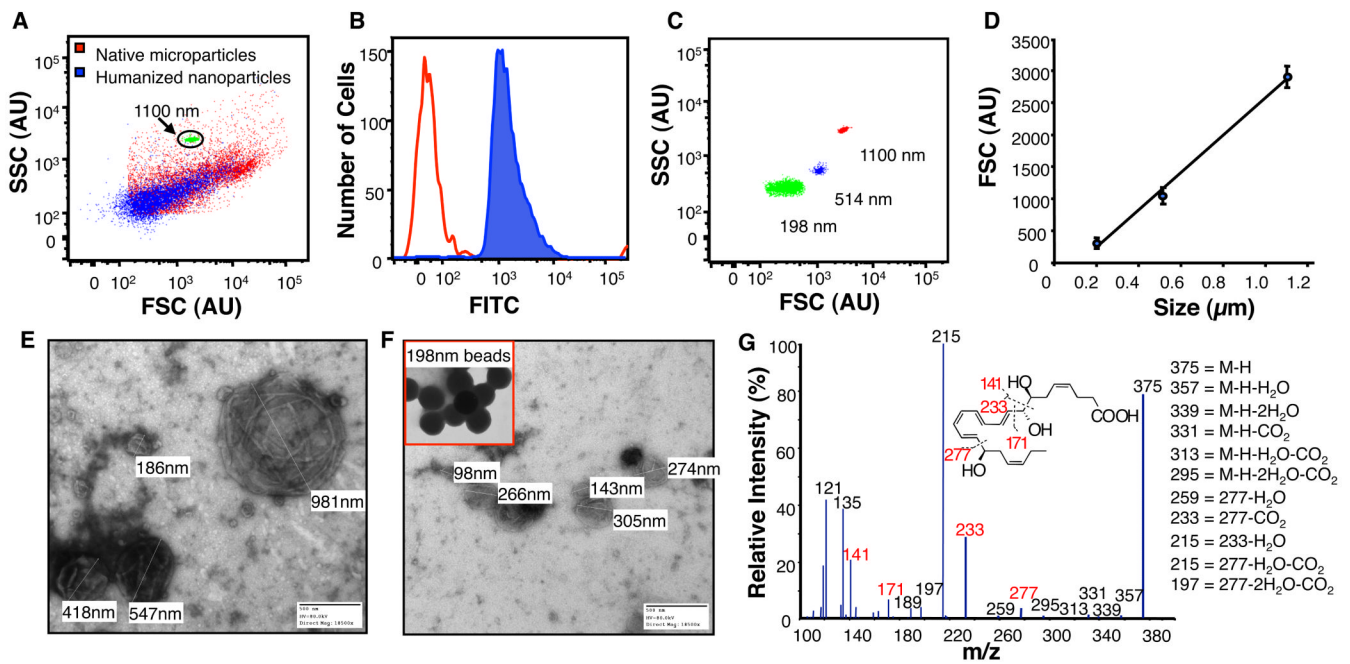


Figure 3. Humanized nano pro-resolving medicines (NPRMs): Construction and characterization

(A) Human PMN-derived MPs (red) were isolated and enriched with AT-RvD1 or α -[9,12]-benzo- ω 6-epi-LXA₄ and fluorescent 1,2-dioleoyl-glycero-3-phospho-L-serine-N (7-nitro-2-1,3-benzoxadiazol-4-yl). Enriched NPRMs were separated by size-exclusion chromatography and sized by flow cytometry (blue). (B) Fluorescence incorporation into NPRM (blue histogram) was monitored by flow cytometry. (C & D) NPRM sizing was determined using cytometry calibration beads. (E & F) Sizing was also validated using electron microscopy of MPs and NPRMs following negative staining, calibration nanospheres are shown inset. (G) Incorporation of AT-RvD1 into NPs was determined using LC-MS/MS with representative mass spectra.

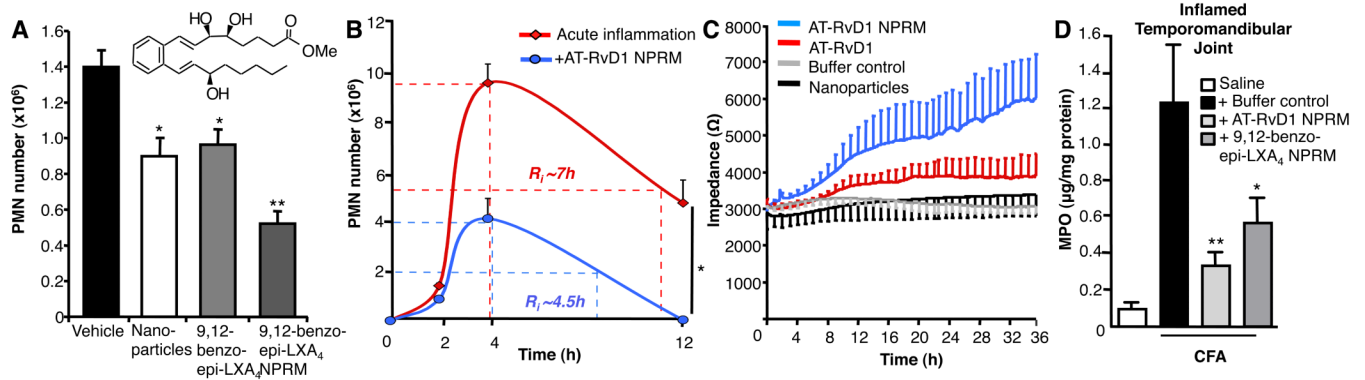


Figure 4. Nano-pro-resolving medicines limit PMN infiltration to inflammatory sites, enhance wound healing and are protective in TMJ

(A) Peritoneal PMN infiltration was assessed 2h after zymosan ($100\mu\text{g}$ i.p.). Mice were treated with vehicle, NPs (1×10^5), LXA₄ analog (300ng), or LXA₄ analog NPRMs (1×10^5). (B) Mice were given vehicle or AT-RvD1 NPRMs (1×10^5 i.v.) before zymosan ($100\mu\text{g}$ i.p.), and the resolution interval (R_i) of acute inflammation was calculated. (C) Wound healing of keratinocytes was assessed *in vitro* following treatment with vehicle, NPs, AT-RvD1 (10 nM) or AT-RvD1 (10 nM) NPRMs ($n=3$). (D) NPRMs limit PMN infiltration to CFA-inflamed TMJs. Mice administered CFA ($10\mu\text{g}$, $20\mu\text{l}$, periarticular) to the left TMJ and saline ($20\mu\text{l}$) into the right TMJ followed by i.v. treatment with buffer ($100\mu\text{l}$ PBS), AT-RvD1 (10ng) NPRMs or LXA₄ analog (10ng) NPRMs, and 12h MPO tissue levels were assessed in CFA-inflamed TMJ ($n=3-7$ per treatment group). Values are mean \pm SEM. * $p < 0.05$, ** $p < 0.01$.